

Radiating Element For Wide Bandwidth Scanned Array Antennas

G. Byrne, J. McCormick
Selex-S&AS, Ferry Road, Crewe Toll,
Edinburgh, EH5 2XS

Abstract

A design approach for a wide bandwidth (multiple-octave) radiating element for scanned array antennas is presented. Evidence that the radiating element feed (transition) was a limiting factor for bandwidth, naturally led to the strategy that to obtain a wide bandwidth radiating element, requires a wide bandwidth transition. The printed Marchand balun is demonstrated to fulfil this requirement and when coupled to a Vivaldi type radiating structure providing the possibility of greater than 5:1 bandwidth with 60° scan away from boresight.

Keywords: Radiating Element, Vivaldi, Balun, Array, Antenna

Introduction

From initial investigations, Tapered Slot Antennas (TSA) were identified as the most promising type of wide bandwidth radiating element for scanned array antennas. It has been widely reported [1, 2, 3] that TSA's can provide multiple octave bandwidth operation over an extremely wide range of scan angles, but typically require a transition from the radiating structure to either stripline or microstrip transmission line, for connection to the feed network or Transmit / Receive Module (TRM) in active electronically scanned arrays (AESA). The transition was therefore identified as a limiting factor in obtaining wide bandwidth performance and a critical constraint in the radiating element design. If a wide-band transition design could be realised it should be possible to design a wide bandwidth radiating element. Selex-SAS has significant experience with Notch and Vivaldi type radiating elements and considering the bandwidth requirements it was decided to select a Vivaldi type element. The TSA's considered also have the added advantage of easy integration with existing AESA technology and architectures.

The Marchand and Double-Y baluns were both considered as possible transitions. Initial modelling concluded that both provided bandwidths of greater than 5:1 and were both suitable for integration with Vivaldi type antennas. The Marchand balun was selected as the candidate transition, since it appeared to offer more easily identifiable parameters that could be used to adjust the operating bandwidth. A simple set of design rules are formulated to aid the design of a Marchand balun. Finally, a "good" Marchand balun transition was coupled to a Vivaldi radiating element and a calculation of the active reflection coefficient in an infinite array environment was performed. It is shown that a VSWR of less than 2:1 ($\approx -10\text{dB}$) was predicted for bandwidths approaching 5:1 and a scan range in excess of 60° over the full bandwidth.

Transition Design (balun)

Printed TSA's are essentially slotline radiating structures and can be realised using microstrip or stripline structures. A transition from slotline to microstrip or stripline is therefore required to connect to the feed network or TRM in an active

phased array antenna. As previously stated, to obtain a multi-octave bandwidth radiating element requires a multi-octave bandwidth transition. Preliminary modelling identified Marchand and Double-Y baluns as candidate transitions based on their potential bandwidths of greater than 6:1 and the fact that they can be easily realised as printed circuits suitable for connection to Vivaldi type antennas. A Balun (balanced-to-unbalanced) is a form of transformer that converts an un-balanced transmission line, microstrip (or stripline), to a balanced transmission line, slotline.

For each type of balun (Marchand and Double-Y) two different configurations were considered (1) stripline-to-slotline and (2) microstrip-to-slotline. The stripline-to-slotline configuration is actually a stripline to bi-lateral slotline since there are identical slots in both ground planes. The printed Marchand and Double Y baluns are presented below in Figure 1 and Figure 2 respectively. The representations shown are for microstrip baluns where the microstrip track is printed on one side of the substrate and the slotline is cut from the ground plane on the other side. The stripline construction is similar but the stripline conductor is sandwiched between the two identical substrates and symmetrical slots etched from the top and bottom ground planes.

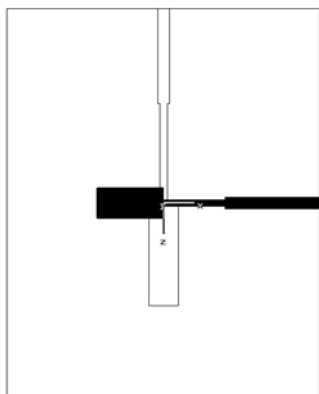


Figure 1 Printed 4th order Marchand Balun

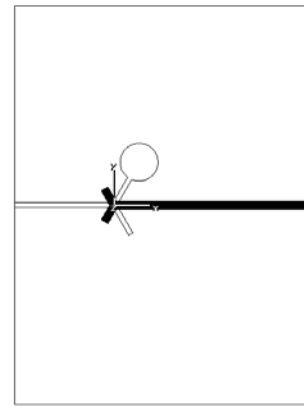


Figure 2 Printed Double-Y Balun

The design strategy adopted was to isolate the transition performance from the radiating element structure and analyse the performance of the transition on its own. By separating the transition from the radiating element structure the process of comparing performance of the candidate transitions was simplified. This process would primarily be used to compare transition performance but it is also anticipated that this would be the first stage in the transition design. Further optimisation of the transition may be possible when the radiating element structure is added to the transition. CST Microwave Studio [5] was used to analyse the transition models and identify the critical parameters. Four basic transitions were modelled: -

- Marchand Balun (4th Order), microstrip-to-slotline (substrate $\epsilon_r = 10.2$)
- Marchand Balun (4th Order), stripline-to-slotline (substrate $\epsilon_r = 2.94$)
- Double-Y Balun, microstrip-to-slotline (substrate $\epsilon_r = 10.2$)
- Double-Y Balun, stripline-to-slotline (substrate $\epsilon_r = 2.94$)

For comparison, two different substrate materials were selected. A high dielectric constant substrate ($\epsilon_r=10.2$) for the microstrip-to-slotline models and a lower dielectric constant substrate ($\epsilon_r=2.94$) for

the stripline-to-slotline models. Each design was then optimised to maximise the bandwidth between 2 and 18GHz with a nominal centre frequency of 10GHz.

The Marchand balun results are presented below in Figure 3. The stripline Marchand balun has a -10dB (less than 2:1) bandwidth of 5.6:1 from 2.9-17GHz compared to the microstrip Marchand balun which has a 5:1 bandwidth from 3.5-17.5GHz. The lower dielectric constant substrate increased the bandwidth with only minor degradation of the in-band match. With further optimisation it may be possible to achieve the full 6:1 bandwidth. The passbands of both baluns demonstrate the characteristic equal-ripple Chebyshev response.

A comparison between the Marchand and Double-Y balun performance is presented for the microstrip-to-slotline configuration in Figure 4. Although broadly similar in terms of return loss, the Marchand balun exhibited a marginally wider bandwidth.

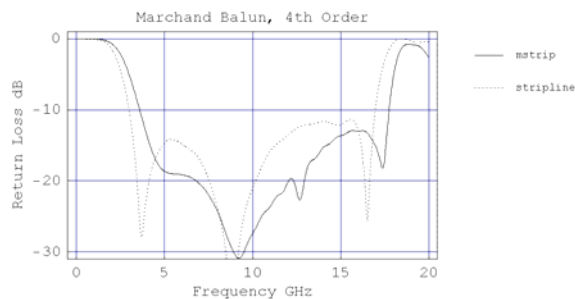


Figure 3 Marchand Balun results for microstrip-to-slotline and stripline-to-slotline transitions

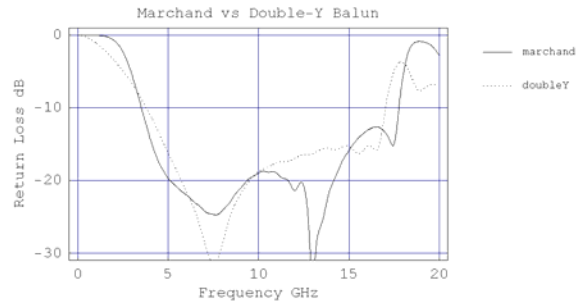


Figure 4 Marchand Balun versus Double-Y Balun for microstrip-to-slotline transition

Marchand Balun Design Rules

The outcome from the electromagnetic modelling was to formulate a simple set of design rules that can be applied to the Marchand balun. The derivation of simple expressions for the design of Marchand baluns, based on distributed TEM networks, was presented by Trifunovic and Jokanovic in [4]. It was shown that a fourth order Marchand balun could be represented by the equivalent circuit given in Figure 5. The impedances Z_0 and R represent the characteristic impedances of the microstrip/stripline and slotline transmission lines in Figure 6. All transmission line lengths are equal to one quarter wavelength ($\lambda_g/4$) at the centre frequency of the passband. Impedances Z_1 and Z_4 are the impedances of the microstrip/stripline and slotline transformer sections and Z_b and Z_{ab} are the impedances of the microstrip/stripline stub and slotline open circuit sections respectively.

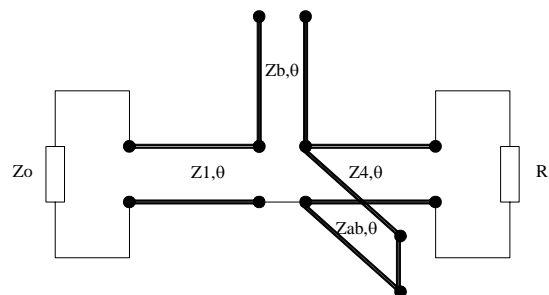


Figure 5 Equivalent circuit for 4th Order Marchand Balun

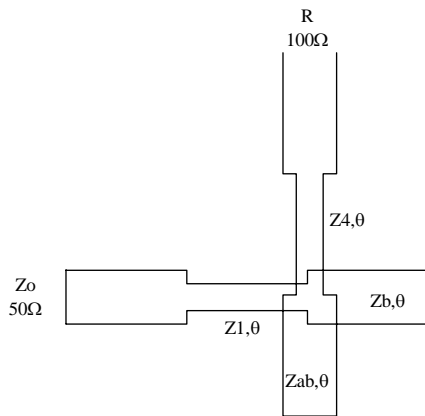


Figure 6 Circuit Schematic of 4th Order Marchand Balun

The Marchand balun exhibits an equal-ripple Chebyshev passband response and can be controlled by the impedances Z_1 , Z_b , Z_{ab} and Z_4 . The theoretical passband characteristics of second, third and fourth order Marchand baluns is shown below in Figure 7, and as can be seen is similar in response to the predicted balun performance shown in Figure 3.

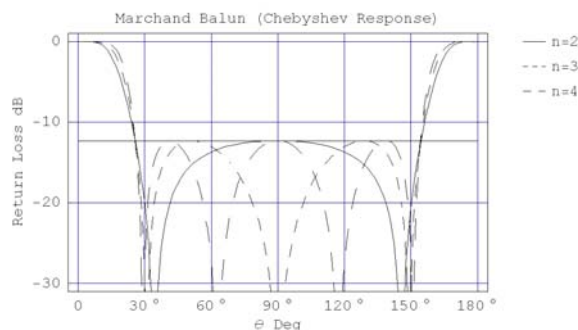


Figure 7 Ideal Chebyshev Passband Characteristic of the Marchand Balun

The design rules for the Marchand balun can be summarised as follows: -

- Select the desired bandwidth (e.g. 2,4,6, or 8:1 etc), and then select the upper and lower frequency limits (' f_u ' and ' f_l ')
- Determine the centre frequency ' f_c ' and calculate the $\frac{1}{4}$ wavelength (guide wavelength) for the slotline

and stripline (or microstrip) sections.

- Select the Marchand balun impedances and calculate the line / gap widths required. Marchand balun impedances can be obtained from the table presented in Table 1, which were calculated from the expressions given in [4]
- The theoretical impedances should produce a design close to the required performance and the final step is to optimise the design by fine tuning the impedances and line lengths

The Marchand balun can then be designed for the desired frequency band, centre frequency and substrate material.

Table 1 Impedances for 4th Order Marchand Balun

Bandwidth B	$Z_1 \Omega$	$Z_b \Omega$	$Z_{ab} \Omega$	$Z_4 \Omega$
2	59.57	70.53	70.89	83.93
4	60.89	42.78	116.89	82.12
6	62.74	31.01	161.26	79.69
8	64.41	24.37	205.21	77.63

Infinite Array Results

This section presents the predicted scan performance of a Vivaldi radiating element in an infinite array environment. A "good" Marchand balun transition design was coupled to a Vivaldi radiating structure to assess scan performance, see Figure 8. A flare length of 15mm was selected in combination with an optimum exponential flare rate of 0.15. The only change required to the balun was the inclusion of a 90 degree bend in the feed line to allow the element to fit the array grid pitch. The active reflection coefficient varies as a function of scan angle due to the variation in mutual coupling as the excitation phase for each element is adjusted and is therefore an important measure of performance. In order to predict the active reflection

coefficient variation with scan angle, the 3D electromagnetic-modelling package Ansoft HFSS [6] was used to define a “unit-cell” using periodic boundaries and control the electronic scan angle (θ_s, ϕ_s) . The radiating element was analysed in a 9.0 x 9.0 mm rectangular grid to obtain a grating lobe free frequency limit of 17.85GHz for 60° scan.

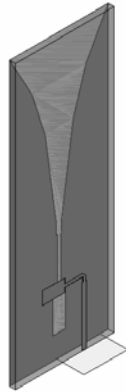


Figure 8 Vivaldi Radiating Element including Marchand Balun transition

The active reflection coefficient has been plotted as a function of frequency and scan angle on a 2D contour plot. All active reflection coefficient plots cover a frequency range of 2-18GHz and scan range of 0-70° in theta for the principal planes (E- & H-plane). The colour scheme chosen has a number of discrete break points at VSWR's of 1.2, 1.5, 2, 2.5 and 3:1. The break points distinguish between different levels of performance, where the white / light grey regions represent “good” performance, less than 2:1, and the dark grey / black regions represent “bad” performance and covers VSWR's from 3:1 to infinity. A second scale has been added to make it easy to convert between VSWR and reflection coefficient (dB). The active reflection coefficient for the E- & H-planes is shown in Figure 9 and Figure 10 respectively. The bandwidth achieved approaches 4:1 (4.5-16GHz) in the E-plane and greater than 4:1 in the H-plane. The E-plane bandwidth was limited by a scan anomaly which appeared lower in

frequency than both the Marchand balun bandwidth and grating lobe limit.

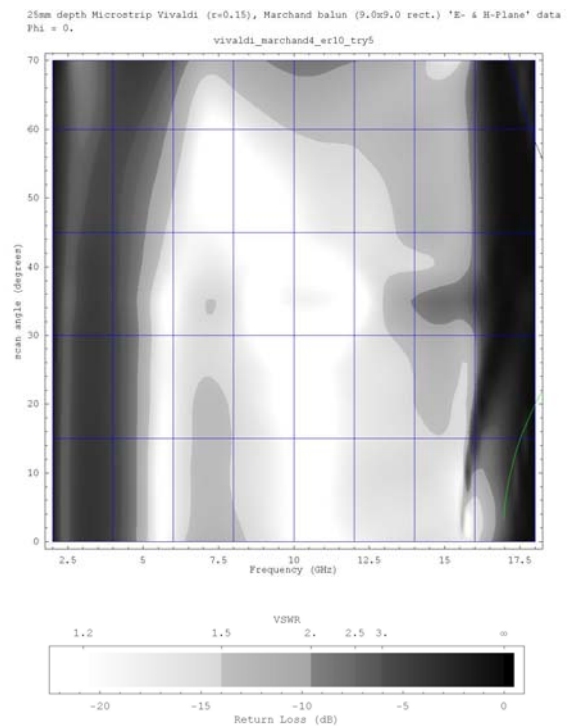


Figure 9 E-Plane Active Reflection Coefficient

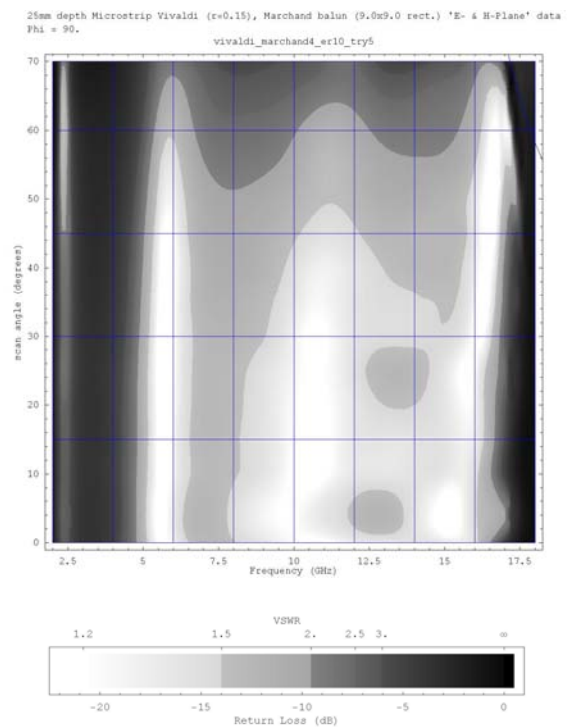


Figure 10 H-Plane Active Reflection Coefficient

However, the H-plane bandwidth was closer to full Marchand balun bandwidth. The active reflection coefficient was extremely well behaved in the passband, with the majority of the frequency / scan range less than 1.5:1 and almost constant with scan angle. Greater than 60° scan was possible over the majority of the frequency range in the E- & H-plane. To increase the bandwidth further would require a reduction in the low frequency limit, however this could be achievable by increasing the flare length.

Conclusions

The printed Marchand balun was identified as a suitable wide bandwidth transition for integration with the selected wide bandwidth radiating element (Vivaldi). It has been shown that the Marchand balun is predicted to be capable of providing a 6:1 bandwidth transition in either stripline or microstrip using a variety of different substrate materials. A simple set of design rules has been formulated so that the Marchand balun can be easily designed for different frequency bands or substrate materials. A lower dielectric constant substrate was seen to improve the balun bandwidth, however there is some evidence (in other results) that the improved bandwidth may be at the expense of resonances due to radiation from the reduced slotline efficiency.

Bandwidths of greater than 4:1 were shown to be possible with Vivaldi radiating elements including the Marchand balun, and it may be possible to optimise the element further to achieve greater than 5:1 bandwidth. Furthermore, greater than 60° scan was possible over almost the entire bandwidth. For the majority of this frequency / scan range a VSWR of less than 1.5:1 was achieved and the VSWR was approximately constant in angle. For this type of element, the boresight performance was therefore a good indicator of the scan

performance. Arrayed elements were also shown to work at surprising low frequencies given the relatively small aperture widths (less than $\lambda_0/8$) and flare lengths ($\lambda_0/4$). At such small grid spacings, the mutual coupling between elements will be significant, but is obviously beneficial in terms of improving the element performance.

References

1. J. Shin and D.H. Schaubert, "A Parameter Study of Stripline-Fed Vivaldi Notch-Antenna Arrays", IEEE Transactions on Antennas and Propagation, Vol.47, No.5, May 1999
2. Tan-Haut Shio and D.H. Schaubert, "Parameter Study and Design of Wide-Band Widescan Dual-Polarised Tapered Slot Antenna Arrays", IEEE Transactions on Antennas and Propagation, Vol.48, No.6, June 2000
3. D.H. Schaubert, "Wide-band Phased Array of Vivaldi Notch Elements", Int. Conf. on Antennas and Propagation, 14-17 April 1997, Page(s) 6-12, Vol. 1
4. V. Trifunovic and B. Jokanovic, "Review of Printed Marchand and Double Y Baluns: Characteristics and Application", Vol.42, No.8, August 1994
5. CST Microwave Studio®, User Manual Version 2006B, Dec.2006, CST Gmbh, Darmstadt, Germany, www.cst.com
6. Ansoft HFSS, Version 10.1.3, Dec 2006, Ansoft Corporation, www.ansoft.com

Acknowledgements

The work reported in this paper was funded by the Electro-Magnetic Remote Sensing (EMRS) Defence Technology Centre, established by the UK Ministry of Defence and run by a consortium SELEX Sensors and Airborne Systems, Thales Defence, Roke Manor Research and Filtronic.